

# Evolution of a neutrino-cooled disc in Gamma-Ray Bursts

A. Janiuk<sup>1,3\*</sup>, R. Perna<sup>2</sup>, T. Di Matteo<sup>3</sup>, B. Czerny<sup>1</sup>

<sup>1</sup>*Nicolaus Copernicus Astronomical Center, Bartycka 18, 00-716 Warsaw, Poland*

<sup>2</sup>*Princeton University, 4 Ivy Lane, Princeton, NJ 08542, USA*

<sup>3</sup>*Max-Planck Institute für Astrophysik, Karl-Schwarzschild-Str. 1, 85740 Garching, Germany*

26 November 2018

## ABSTRACT

Rapid, hyper-Eddington accretion is likely to power the central engines of gamma-ray bursts (GRBs). In the extreme conditions of densities and temperatures the accreting torus is cooled by neutrino emission rather than by radiation. Another important cooling mechanism is the advection of energy into the central black hole. We compute the time evolution of a neutrino-dominated disc that proceeds during the burst and investigate the changes in its density and temperature. The discrimination between short and long bursts is made on the basis of the different rates of material inflow to the outer parts of the disc, thus favoring the binary merger scenario for the short GRBs and the collapsar scenario for the long ones. Within the context of the collapsar model, we also study the evolution of the photon luminosity of the remnant disc up to times  $\sim$  day, and discuss its implications for the production of emission lines in GRB spectra.

**Key words:** accretion, accretion discs – black hole physics – gamma rays: bursts – neutrinos

## 1 INTRODUCTION

In the current view, GRBs are thought to be produced in relativistic ejecta that dissipate energy by internal shocks (Rees & Meszaros 1994). However, other gamma-ray production mechanisms have also been proposed; these include magnetic field reconnections (Drenkhahn & Spruit 2002; Sikora et al. 2003) in Poynting-flux dominated explosions (Lyutikov & Blandford 2003), thermal photospheric emission (Paczynski 1986; Thompson 1994), Compton drag (Lazzati et al. 2000) or photon-pair cascades and multiple Compton scatterings (Stern 2003). The proposed origin of the relativistic ejecta invokes the birth of a black hole in a catastrophic event. This is thought to take place after the merger of two neutron stars or a neutron star and a black hole (Eichler et al. 1989; Paczyński 1991; Narayan, Paczyński & Piran 1992) or in a “collapsar” (Woosley 1993; Paczyński 1998). Both these models involve a stage in which the black hole is surrounded by a debris torus of a large mass, rapidly accreting onto it. The most efficient cooling mechanism for the dense torus is provided by neutrino emission, and neutrino annihilation seems to be an important process for the fireball generation (even though it occurs on timescales that are typically too short to provide the bulk of the GRB energy; e.g. Ruffert & Janka 1999; 2001 but see also Setiawan, Ruffert & Janka 2004).

The durations,  $T$ , of GRBs range from milliseconds to over a thousand of seconds, and are distributed in two distinct peaks that constitute two GRB classes: short ( $T \lesssim 2$  sec) and long bursts ( $T \gtrsim 2$  sec; Kouveliotou et al. 1993). For the long bursts, signatures of an accompanying supernova explosion have been detected in the afterglow spectra (Stanek et al. 2003). This strongly favors the “collapsar” interpretation for their origin. Furthermore, the GRB positions inferred from the afterglow observations are consistent with the GRBs being associated with the star forming regions in their host galaxies. However, all the observations that we have of the GRBs counterparts, i.e. afterglows and host galaxies, have been obtained for the long bursts (see the review by Zhang & Meszaros 2003) and no such signatures have been observed in the case of short bursts. Therefore the merger model is still thought to be viable for the case of short bursts, the nature of which remains mysterious.

In the merger scenario, the duration of the GRB event is much longer than the dynamical timescale but rather comparable to the viscous timescale of the accretion disc. Therefore the phase of accretion sets the burst duration, differently from the collapsar model where there is an external reservoir of stellar matter which feeds the accretion torus. In general, accretion discs in the context of GRBs are expected to have typical densities of the order of  $10^{10-12}$  g cm<sup>-3</sup> and temperatures of  $10^{11}$  K within 10 – 20 Schwarzschild radii ( $R_S = 2GM/c^2$ ). Thus, the accretion proceeds with rates of a solar to several solar masses per second.

\* E-mail: agnes@camk.edu.pl

In this “hyper-accreting” regime, photons become trapped and are not efficient at cooling the disc. Neutrinos, however, are produced by weak interactions in the very dense and hot plasma (“neutrino-dominated accretion flow”, NDAF, Popham Woosley & Fryer 1999; Narayan, Piran & Kumar 2001; Kohri & Mineshige 2002; Di Matteo, Perna & Narayan 2002).

In this paper we compute the time-dependent evolution of a massive accretion disc. We perform our calculations both within the context of a compact object merger scenario and in the collapsar model, where the external supply of a matter, e.g. from the fallback from a supernova explosion (MacFayden, Woosley & Heger 2001), is essential to extend the burst duration into the range appropriate for long bursts. We investigate the evolution of the disc dominated by neutrino cooling, and study the changes of neutrino and photon luminosities with time. In particular, we focus our discussion with the long term evolution (few tens of hours) of these discs and its implication for emission line models reported in the early X-ray afterglow of several GRBs. Our work is thus complementary to the 3D (or 2D) time-dependent numerical studies of Setiawan et al. (2004) and Lee & Ramirez-Ruiz (2002) in being able to extend to the study of the evolution of the bursts (in both collapsar and merging scenario) to much longer timescale. The paper is organized as follows. In Section 2 we describe the basic assumptions of the model of hyper-Eddington accretion disc and the method used in time-dependent numerical simulations. In Section 3 we show the evolution of the disc density and temperature, as well as the resulting neutrino luminosity. In Section 4 we discuss the implications of the long term evolution of the accretion disc for models of line production in GRB afterglow spectra. Finally, we summarize our results in Section 5.

## 2 METHOD

The structure of a steady-state, neutrino-dominated accretion flows (NDAFs) has recently been studied by Popham, Woosley & Fryer (1999), Kohri & Mineshige (2002) and Di Matteo, Perna & Narayan (2002). Here we use a similar prescription to calculate the initial disc configuration, which afterwards is subject to viscous evolution.

### 2.1 Assumptions and model parameters

Throughout our calculations we use the vertically integrated equations of the disc structure, however we note, that in most of the cases the disc becomes moderately geometrically thick ( $H \sim 0.5r$ ). We assume that the disc extends not further out from the central black hole than  $50 R_S$ , as shown e.g. in the recent simulations performed by Rosswog, Speith & Wynn (2004). If the disc size were larger, the flow would become highly convection-dominated instead of forming an NDAF (Narayan, Piran & Kumar 2001). The initial mass of such a disc is  $M_{\text{disc}} \sim 4\pi R_{\text{out}}^3 \Sigma_{\text{out}}$ , which is  $\approx 0.35 M_\odot$  for the accretion rate  $\dot{M} = 1 M_\odot/\text{s}$ . The angular velocity of the disc is assumed to be Keplerian,  $\Omega = \sqrt{GM/r^3}$ , and the sound speed is  $c_s = \sqrt{P/\rho} = \Omega H$ . A non-rotating, Schwarzschild black hole is assumed and the inner radius of the disc is always at  $3 R_S$ .

For the disc heating we use the standard  $\alpha$  viscosity

prescription of Shakura & Sunyaev (1973) and we adopt a canonical value of  $\alpha = 0.1$ . The total pressure  $P$  consists of the gas and radiation pressure as well as the pressure of degenerate electrons:

$$P = P_{\text{rad}} + P_{\text{gas}} + P_{\text{deg}} \quad (1)$$

$$P_{\text{gas}} = \frac{k}{m_p} \rho T \left( \frac{1}{4} + \frac{3}{4} X_{\text{nuc}} \right) \quad (2)$$

$$P_{\text{rad}} = \frac{11}{12} a T^4 \quad (3)$$

$$P_{\text{deg}} = \frac{2\pi\hbar c}{3} \left( \frac{3}{8\pi m_p} \right)^{4/3} \left( \frac{\rho}{\mu_e} \right)^{4/3} \quad (4)$$

where we take the mass fraction of free nucleons  $X_{\text{nuc}} = 30.97(\rho/10^{10})^{(-3/4)}(T/10^{10})^{(9/8)} \exp(-6.096/T/10^{10})$  if  $X_{\text{nuc}} < 1.0$  and  $X_{\text{nuc}} = 1.0$  elsewhere, and we assume the molecular weight per electron  $\mu_e = 2$ . The radiation pressure includes the contribution from the electron-positron pairs via the coefficient  $11/12$ . The radiation pressure is always taken into account in the hydrostatic balance and thermodynamic relations, however we neglect it in the viscous heating. Therefore we have:

$$Q_{\text{visc}}^+ = \frac{3}{2} \alpha \Omega H (P_{\text{gas}} + P_{\text{deg}}). \quad (5)$$

The cooling in the disc is due to advection, radiation and neutrino emission. The advective cooling in a stationary disc is determined from the global ratio of the total advected flux to the total viscously generated flux (e.g. Paczyński & Bisnovatyi-Kogan 1981; Muchotrzeb & Paczyński 1982; Abramowicz et al. 1988):

$$Q_{\text{adv}}^- = \frac{F_{\text{adv}}}{F_{\text{tot}}} = -\frac{2r P q_{\text{adv}}}{3\rho G M} \quad (6)$$

and

$$q_{\text{adv}} = (12 - 9\beta) \frac{\partial \ln T}{\partial \ln r} - (4 - 3\beta) \frac{\partial \ln \rho}{\partial \ln r}. \quad (7)$$

Here  $\beta$  is the ratio of the gas plus degeneracy pressure to the total pressure  $\beta = (P_{\text{gas}} + P_{\text{deg}})/P$ . In the initial stationary disc we assume that  $q_{\text{adv}}$  is approximately constant and of order of unity, but in the subsequent time-dependent evolution the advection term is calculated more carefully, with appropriate radial derivatives.

In case of photon and electron-positron pairs in the plasma the radiative cooling is equal to:

$$Q_{\text{rad}}^- = \frac{3P_{\text{rad}} c}{4\tau} = \frac{11\sigma T^4}{4\kappa \Sigma} \quad (8)$$

where we adopt the Rosseland-mean opacity  $\kappa = 0.4 + 0.64 \times 10^{23} \rho T^{-3} \text{ cm}^2/\text{g}$ .

The most significant neutrino emission processes are:  $\dot{q}_{\text{Ne}} = 9 \times 10^{33} (\rho/10^{10})(T/10^{11})^6 X_{\text{nuc}} \text{ ergs/cm}^3/\text{s}$ , the cooling rate in the non-degenerate URCA process (Qian & Woosley 1996);  $\dot{q}_{e^+e^-} = 4.8 \times 10^{33} (T/10^{11})^9 \text{ ergs/cm}^3/\text{s}$ , the emission due to the electron-positron pair annihilation (Itoh et al. 1989);  $\dot{q}_{\text{brems}} = 1.5 \times 10^{27} (T/10^{11})^{5.5} (\rho/10^{10})^2 \text{ ergs/cm}^3/\text{s}$  is the the bremsstrahlung emission in the non-degeneracy regime of nucleons (Hannestad & Raffelt 1998) and  $\dot{q}_{\text{plasmon}} = 1.5 \times 10^{32} (T/10^{11})^9 f(\gamma_p) \text{ ergs/cm}^3/\text{s}$  is the plasmon decay rate (Ruffert, Janka & Schäfer 1996). The largest contribution to the neutrino emission is due to the electron capture on nucleons  $\dot{q}_{\text{Ne}}$ . The electron-positron annihilation rate could be neglected in the case of complete

degeneracy of electrons, i.e. for  $\lambda_e/kT \gg 1$ , where  $\lambda_e$  is the chemical potential of electrons. However, in the subsequent calculations the degeneracy parameter is never extremely large, and therefore  $\dot{q}_{e^+e^-}$  is also taken into account.

In the above processes either electron flavor neutrinos and antineutrinos are produced (URCA process, plasmon decay), or all the neutrino flavors, including the heavy lepton neutrinos and antineutrinos (pair annihilation, bremsstrahlung). In this work we further neglect the possible anisotropies between neutrinos and antineutrinos as well as between different flavors, that could arise e.g. from a multiflavour neutrino leakage scheme (e.g. Rosswog & Liebendörfer 2003).

We treat, in a simplified scheme, neutrino cooling both in the optically thin and optically thick regimes.

In the (i) *optically thin regime* the cooling is simply given by:

$$Q_\nu^- = H(\dot{q}_{Ne} + \dot{q}_{e^+e^-} + \dot{q}_{\text{brems}} + \dot{q}_{\text{plasmon}}). \quad (9)$$

In the (ii) *optically thick regime* we include in our calculations the prescription for the neutrino opacity according to Di Matteo et al. (2002). This will allow us to switch smoothly between the optically thick and thin regimes. Each neutrino emission process described above has an inverse process corresponding to absorption. Absorption onto protons or onto neutrons (the inverse of the URCA process) gives rise to the large majority of the (a) *absorptive optical depth*, thus given by (see Di Matteo et al. 2002 for details):

$$\tau_{\text{abs}} = \frac{\dot{q}_{Ne}H}{4 \times (7/8)\sigma T^4} = 4.5 \times 10^{-7} (T/10^{11})^2 X_{\text{nuc}} (\rho/10^{10}) H. \quad (10)$$

A very important contribution to the overall opacity for all neutrino species comes from neutral-scattering off nucleons. The (b) *scattering optical depth* is given by (see Di Matteo et al. 2002 for derivation of scattering optical depth):

$$\tau_{\text{sc}} = 3\rho\kappa_s H = 8.1 \times 10^{-7} (T/10^{11})^2 (\rho/10^{10}) H \quad (11)$$

where the factor 3 assumes equal contribution for all neutrino species, i.e. thermal equilibrium.

The neutrino cooling in this case is then given by:

$$Q_\nu^- = \frac{7}{8}\sigma T^4 \left( \frac{\tau_{\text{abs}} + \tau_{\text{sc}}}{2} + \frac{1}{\sqrt{3}} + \frac{1}{3\tau_{\text{abs}}} \right). \quad (12)$$

In addition, in this regime, the equation of state should contain the neutrino pressure:

$$P_\nu = \frac{1}{3} \times \frac{7}{8} a T^4 \frac{\frac{\tau_{\text{abs}} + \tau_{\text{sc}}}{2} + \frac{1}{\sqrt{3}}}{\frac{\tau_{\text{abs}} + \tau_{\text{sc}}}{2} + \frac{1}{\sqrt{3}} + \frac{1}{3\tau_{\text{abs}}}} \quad (13)$$

Finally, the entropy density due to neutrinos,  $S_\nu = 4/3 \times 7/8 a T^4$ , is included in the advective cooling when we calculate the initial disc configuration.

The last equation that is essential to close our set of equations for the stationary disc is the total energy flux  $F_{\text{tot}}$ . It is dissipated within the disc at a radius  $r$  and is determined by the global parameters:

$$F_{\text{tot}} = \frac{3GM\dot{M}}{8\pi r^3}. \quad (14)$$

(Note, that the above equation will not be used in the subsequent time-dependent calculations.) In order to calculate the initial stationary configuration, we solve the energy balance:

$F_{\text{tot}} = Q_{\text{visc}}^+ = Q_{\text{adv}}^- + Q_{\text{rad}}^- + Q_\nu^-$ . In this energy balance we did not include the cooling term due to the photodisintegration (Di Matteo et al. 2002), while we include the radiative cooling. We checked that this term is much less than the neutrino cooling rate in the innermost parts of the disc, when the hot disc is cooled by neutrinos, and less than advective and radiative cooling, when these two mechanisms start playing important role.

The initial configuration of the disc is calculated by means of a simple Newtonian method. This lets us determine the radial profiles of density and temperature, as well as the disc thickness and opacity at time  $t = 0$ .

## 2.2 Time evolution

In the previous subsection we described the initial, stationary disc configuration. Having computed the initial disc state we allow the density and temperature to vary with time. We solve the time-dependent equations of mass and angular momentum conservation for such a disc:

$$\frac{\partial \Sigma}{\partial t} = \frac{1}{r} \frac{\partial}{\partial r} (3r^{1/2} \frac{\partial}{\partial r} (r^{1/2} \nu \Sigma)) \quad (15)$$

and the energy equation:

$$\begin{aligned} \frac{\partial T}{\partial t} + v_r \frac{\partial T}{\partial r} = & \frac{T}{\Sigma} \frac{4 - 3\beta}{12 - 9\beta} \left( \frac{\partial \Sigma}{\partial t} + v_r \frac{\partial \Sigma}{\partial r} \right) \\ & + \frac{T}{PH} \frac{1}{12 - 9\beta} (Q^+ - Q^-). \end{aligned} \quad (16)$$

Here  $\Sigma = H\rho$  is the surface density and  $v_r \approx (3\nu)/(2r)$  is the radial velocity in the disc,  $\nu = (2P\alpha)/(3\rho\Omega)$  is the kinematic viscosity. The cooling term  $Q^-$  consists of radiative and neutrino cooling, given by Equations 8 and 9 (or 12). The advection is included in the energy equation via the radial derivatives. In the heating term  $Q^+$  we include gas and degeneracy pressure (in the optically thin regime) and also neutrino pressure (in the optically thick regime). Note, that this equation includes the radiation entropy, via the coefficient  $\beta$ , which is not equal to unity due to the presence of radiation pressure in the total pressure.

We solve the above set of time-dependent equations using the convenient change of variables,  $y = 2r^{1/2}$  and  $\Xi = y\Sigma$ , at the fixed radial grid, equally spaced in  $y$  (see Janiuk et al. 2002 and references therein). The number of radial zones is set to 20. After determining the solutions for the first 100 time steps by the fourth-order Runge-Kutta method, we use the Adams-Moulton predictor-corrector method, allowing the time-step to vary, when needed.

We choose the no-torque inner boundary condition,  $\Sigma_{\text{in}} = T_{\text{in}} = 0$  (see Abramowicz & Kato 1989). The outer boundary of the disc is parameterized by an external accretion rate  $\dot{M}_{\text{ext}}$  in case of the collapsar scenario.

In case of the merging compact objects scenario there is no matter supply to the disc, and we can have  $\Sigma_{\text{out}} = T_{\text{out}} = 0$ . However, the outer edge of the disc should expand to conserve the angular momentum, and in principle the density would vanish at the infinite distance. In order to satisfy this requirement, we supplement our radial grid with 10 empty rings between 50 and 96  $R_S$ , while the outer boundary condition  $\Sigma = T = 0$  is located at 96  $R_S$ . These empty rings gradually fill with material that sinks from the outermost disc radius by means of the viscous diffusion, and

take the angular momentum from the disc. The extension of the empty zone is large enough to ensure that at the end of the calculations the surface density in N-1 ring is less than 5% of the surface density in the zone 20 (the edge of the initial disc).

### 3 RESULTS

We first analyze the local evolution of the disc on the  $T - \Sigma$  plane, and then we show examples of time evolution of the neutrino luminosity for a chosen set of parameters.

#### 3.1 Stability curves

A few examples of stability curves calculated at 4, 10, 20 and 46  $R_S$  for the mass of the central object equal  $3M_\odot$  are shown in Figure 1. The open points represent the stationary solutions, calculated from the grid of steady-state models (optically thin regime). The solid points represent the subsequent solutions of the time-dependent model. Deviation between the stationary and time-dependent solutions arises from the simplified description of advection, used in the stationary model. In that model we had a constant value of the advection parameter given by Eq. 7:  $q_{adv} = 1.0$  and does not depend on radius, while in the time dependent model the radial derivatives are calculated properly. However, this simplification of the stationary model does not influence the time-dependent results, since we start the evolution from the upper, neutrino-cooled branch, where advection term is not crucial.

We see that the resulting curves display the pattern already discussed in Kohri & Mineshige (2002). Both upper and lower branches of different slopes are viscously and thermally stable. On the upper branch the dominant cooling mechanism is the neutrino cooling, and the radiation pressure is much lower than gas and degeneracy pressures (most of this branch is in fact gas-pressure dominant, and the degeneracy pressure can exceed it only for very large densities,  $\rho > 3 \times 10^{12} \text{ g/cm}^3$ ). On the lower branch the radiation pressure dominates, however the flow is cooled by advection rather than radiation, and therefore the disc should remain stable. Below this branch, for much lower densities and temperatures, we expect the unstable (radiatively cooled and radiation pressure dominant) branch to appear, as shown in detail by Pringle, Rees & Pacholczyk (1974) and Lightman & Eardley (1974).

We start the disc evolution from the top of the upper branch, and first we let it cool down very quickly due to the zero mass inflow at the outer edge. In the initial configuration, neutrino cooling is dominant in the entire disc. Although the outer boundary condition imposes a fast density decrease at the outer edge of the disc, the inner parts do not respond immediately to that. For the first  $\sim 1$  second the disc annuli evolve slowly along the upper branch, and the density of the disc decreases as the matter falls into the black hole. In this branch the temperature changes are not very significant, so it is the substantial density evolution that drives the steep fall of the disc luminosity.

The evolution starts to proceed faster when all the disc annuli find themselves on the lower branch, where advective cooling becomes dominant. As the whole disc is dominated

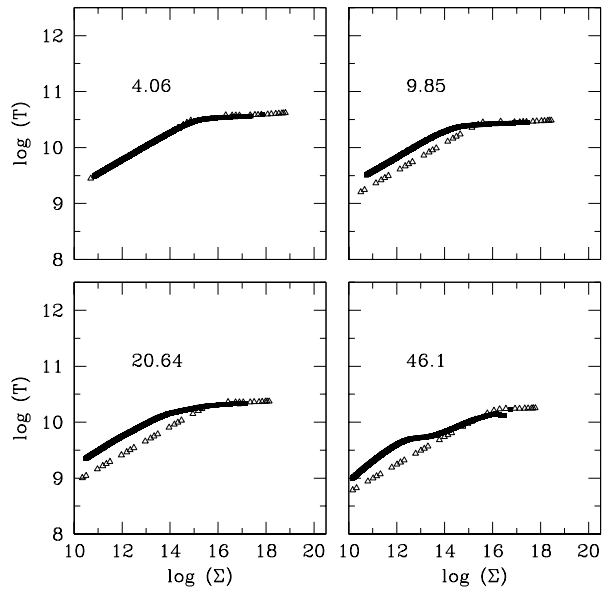


**Figure 1.** Local evolution of the disc on the surface density - temperature plane, plotted for 4 values of radius: 4.06, 9.85, 20.64 and 46.1  $R_S$ , in case of the disc optically thin to neutrinos. The open triangles mark the stability curve resulting from stationary disc solutions. The solid points are the time-dependent solutions.

by advective cooling, we reach the so-called slim disc branch. Here the radiation pressure is larger than gas and degeneracy pressure. As a result of this, we may expect the outer edge to develop an instability leading to the disc break down, if the viscous heating was assumed proportional to the total (gas and radiation) pressure. On the other hand, if the viscous heating is assumed proportional only to the gas pressure, there is no problem with instabilities during the slim disc evolution. Therefore we choose this prescription, also having in mind the recent results of 3-D simulations performed by Turner (2004), which show that the radiation pressure instability is strongly suppressed when the angular momentum transport in the accretion disc is described by MHD calculations, without the  $\alpha$  parameter. This heating prescription makes no difference at the NDAF branch, where more important contribution is given by gas, degeneracy and neutrino pressure, which we always take into account. Since neutrino cooling is no longer important ( $L_\nu < 10^{50} \text{ ergs/s}$ ), further calculations would not be relevant for the study of GRB central engine and we stop our calculations here.

The disc evolution proceeds much slower when the accretion rate at the outer edge is non-zero. The phase of the most efficient neutrino cooling, i.e. when the innermost disc parts are cooled mainly by the neutrino emission and not by advection, is extended to  $\sim 10$  seconds. Also the second phase, of the advection-dominated disc, is much longer. The disc evolves along the advective branch more slowly and there is no rapid emptying of the outer parts.

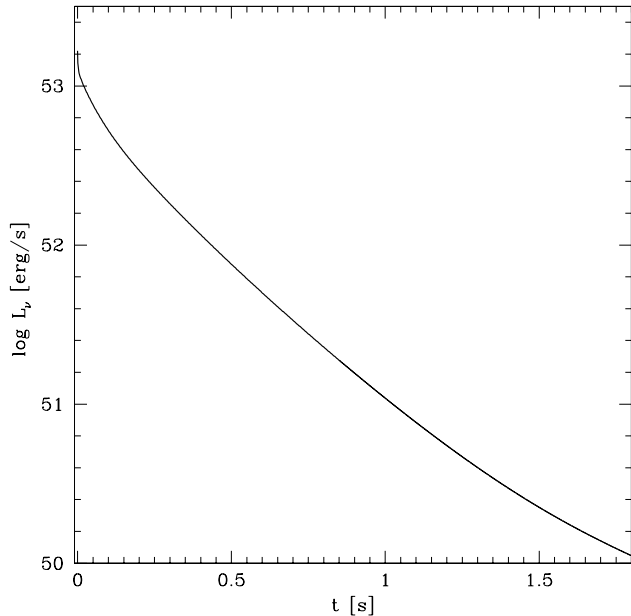


**Figure 2.** The time evolution of the neutrino luminosity in case of no external mass supply to the disc (optically thin case). The initial accretion rate is  $\dot{M} = 1 M_{\odot}/s$ .

### 3.2 Lightcurves

The outer boundary condition for the disc evolution depends on the accretion rate,  $\dot{M}_{\text{ext}}$ . If we assume that the torus was formed during the merger of two compact objects, NS-NS or BH-NS, it will consist of the debris matter from the disrupted neutron star and there will be no source of additional material infalling onto the disc. On the other hand, if we take into account the “collapsar” model, the associated supernova explosion should provide a declining fallback of matter, that accumulates mostly in the equatorial plane. The variations of the mass supply to the accretion flow will strongly influence the disc evolution and therefore result in significant changes in the lightcurves.

The lightcurves represent the neutrino luminosity of the disc. The luminosity is given by:

$$L_{\nu} = \int_{R_{\min}}^{R_{\max}} Q_{\nu}^{-} 2\pi r dr \quad (17)$$

where  $Q_{\nu}^{-}$  is given by either Equation 9 or 12 as appropriate for the optically-thin and thick regimes.

#### 3.2.1 Optically thin regime

In Figure 2 we show an example of a neutrino lightcurve calculated under the assumption of an optically-thin neutrino disc for the case of zero mass supply. Other parameters were always the same: mass of the central object  $M = 3M_{\odot}$ ,  $\alpha = 0.1$ ,  $R_{\text{out}} = 50R_S$ , and the starting accretion rate was  $\dot{M}_0 = 1 M_{\odot}/s$ .

In Figure 3 we show the neutrino lightcurve calculated for the case of additional matter supply at the outer edge of the disc, which declines with time as:

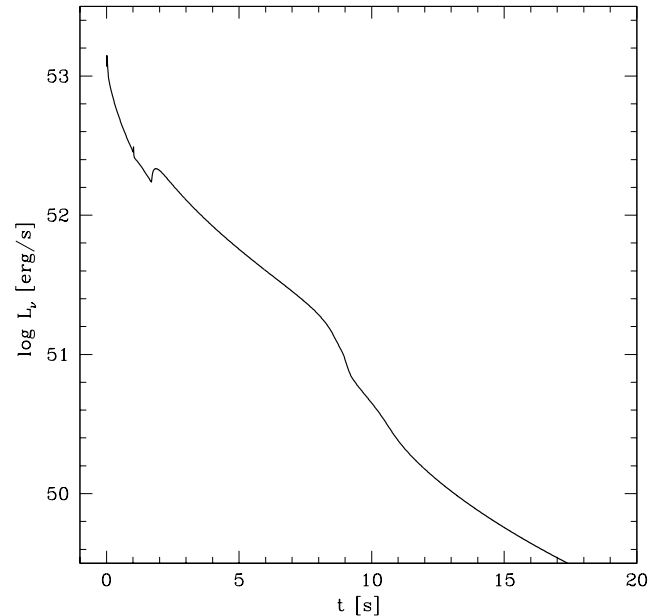


**Figure 3.** The time evolution of the neutrino luminosity in case of additional external mass supply to the disc, declining with time as in the canonical supernova fallback prescription,  $\dot{M}_{\text{ext}} \sim t^{-5/3}$ . The initial accretion rate is  $\dot{M} = 1 M_{\odot}/s$ . The disc is optically thin to neutrinos.

$$\dot{M}_{\text{ext}} = \dot{M}_0 t^{-5/3} \quad (18)$$

This is the time dependence of the fallback of material derived for the supernova SN 1987A (Chevalier 1989) and we adopt it as a canonical rate of the fallback in case of GRBs associated with supernovae. The starting accretion rate was again  $\dot{M}_0 = 1 M_{\odot}/s$ .

Clearly, the supply of material at the outer edge of the disc extends the duration of the hot phase, when the neutrino cooling dominates. GRBs associated with a supernova explosion can therefore have much longer durations, of the order of tens of seconds, depending on the initial mass of the disc and accretion rate. The neutrino luminosity declines exponentially, with some slight luminosity fluctuations in the initial phase, when the neutrino cooling remains dominant at least in the innermost disc parts. The lightcurve smoothens as soon as the whole disc switches to the advection-dominated mode, but its slope does not change much.

#### 3.2.2 Optically thick regime

When the disc is optically thin to its neutrino emission, the cooling rate due to neutrinos,  $Q_{\nu}^{-}$ , is given by Equation 9. However, the disc can become optically thick to neutrinos, especially in its innermost regions and for high accretion rates. The optical depth is larger than unity in the initial disc state. Although it drops very fast in the outer disc radii, still remains quite high for most of the disc evolution in the innermost parts. In this case the cooling rate due to neutrinos  $Q_{\nu}^{-}$  is given by Equation 12.

In Figure 4 we show the neutrino luminosity resulting from the model in which we include the treatment of neu-

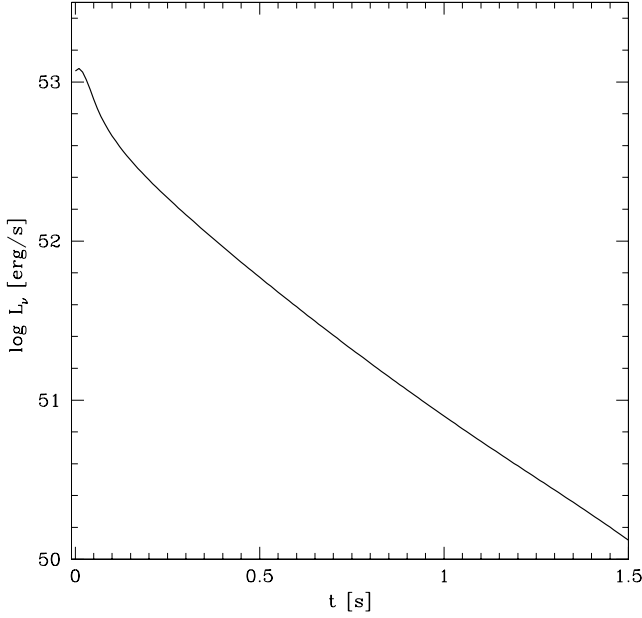


**Figure 4.** The time evolution of the neutrino luminosity in case of no external mass supply to the disc and neutrino optical depth included in the model. The initial accretion rate is  $\dot{M} = 1 M_{\odot}/s$ .

trino optical depths and add the neutrino pressure term in the equations. As expected, the most significant change in comparison with the optically thin case (Figure 2) occurs at the very beginning of the evolution, when the innermost disc is optically thick to its neutrino emission. After about 0.2 seconds most of the disc becomes optically thin to neutrinos and the solution is almost the same as in Section 3.2.1.

Recently, Lee et al. (2004) computed the dynamical simulation of a short GRB, resulting from the merger of two neutron stars. They showed that inclusion of the neutrino optical depth influences the duration and variability of the short burst. Our simulation confirms this conclusion: in Figure 5 we show the comparison of the neutrino luminosity evolution in the optically thin and thick regimes, in the zoom-in emphasizing the shortest timescale by means of the logarithmic units. As the figure shows, in the optically thick case the neutrino luminosity around 20 milliseconds is enhanced, consistently with Lee et al. simulations. Then, the luminosity declines slightly steeper than for the thin disc and the duration of the burst is shorter.

In Figure 6 we plot the disc evolution on the surface density vs. temperature plane in case of the disc optically thick to neutrinos. The main difference in comparison to the optically thin case (Figure 1) is at the inner radii, where the local solutions achieve higher temperatures,  $T > 10^{11} K$ . Further out, and also later in time, when the disc becomes advective and neutrino optical depth is less than 1.0, the solutions match the optically thin case.

In case of a long burst, the difference between the optically thin and optically thick regimes is not significant, since after  $\sim 1$  second of the disc evolution the both optical depths  $\tau_{\text{abs}}$  and  $\tau_{\text{sc}}$  become less than 1.0 and we can substitute the optically thick equations with the optically thin ones. Thus,

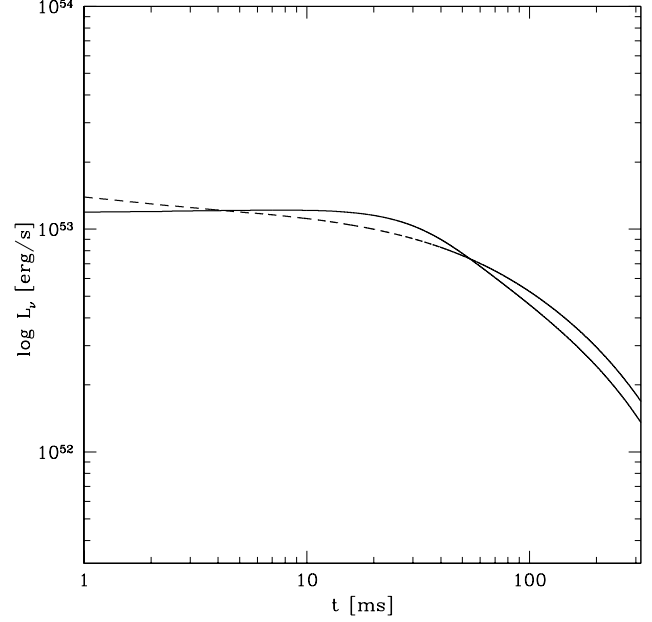


**Figure 5.** The time evolution of the neutrino luminosity in case of no external mass supply to the disc (compact objects merging scenario). The solid line shows the model with neutrino optical depth, while the dashed line is the optically thin case. The initial accretion rate is  $\dot{M} = 1 M_{\odot}/s$  and  $\alpha = 0.1$ .

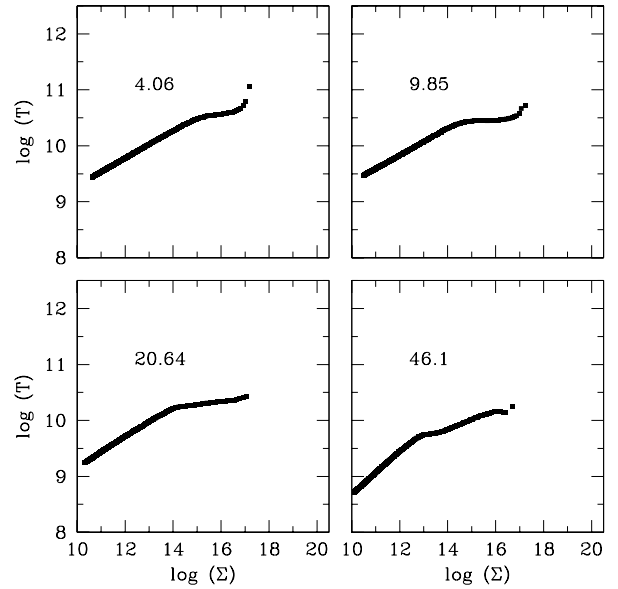


**Figure 6.** Local evolution of the disc on the surface density - temperature plane, plotted for 4 values of radius: 4.06, 9.85, 20.64 and 46.1  $R_S$ , in case of the neutrino-thick inner disc. The points are the time-dependent solutions, for the time range 0 - 0.4 seconds.

in practice, the resulting lightcurve does not differ from that shown in Figure 3.

#### 4 LONG-TERM EVOLUTION OF THE ACCRETION DISC AND ITS IMPLICATIONS FOR EMISSION LINE MODELS

Our time-dependent code allows us to follow the evolution of the GRB accretion disc up to times much longer than the duration of the GRB itself. This is valuable information in light of the peculiarities observed in the early stages of some afterglows (e.g. Fox et al. 2003), which hint at a more extended period of energy injection than the GRB phase itself. What is however particularly relevant for, is the interpretation of the narrow emission features that have been reported in the early X-ray afterglow of several bursts (Yoshida et al. 1999; Antonelli et al. 2000; Piro et al. 1999, 2000; Reeves et al. 2002). Although the statistical significance of the detections is not compelling, the interpretation of these lines bears important implications for our understanding of GRB progenitors.

The emission lines are detected at the rest frame frequency of the host galaxy, and therefore they cannot be produced within the fireball, which, during the X-ray afterglow phase, is still moving towards the observer at a very high speed, with a Lorentz factor  $\Gamma \gtrsim 10$ . Any emission model for the lines must be confronted (as a minimum requirement) with the energetics of the lines, which have a luminosity (for isotropic emission)  $\sim 10^{44} - 10^{45}$  erg/s and last for several hours. This luminosity values must be augmented by a factor  $1/\eta$ , where  $\eta$  is the efficiency for the reprocessing of the impinging flux into line photons. The efficiency of conversion of the X-ray ionizing continuum into  $K_\alpha$  line photons was investigated by Lazzati et al. (2002). They assumed that the line is produced by reflection off an optically thick slab of material, illuminated by a power-law continuum. Under these conditions, which provide the most efficient way of reprocessing continuum photons into  $K_\alpha$  lines, they found that the efficiency  $\eta$  can be at most 2%. This implies that the impinging continuum flux must carry an energy  $\gtrsim 10^{46} - 10^{47}$  erg/s.

This energy requirement could in principle be alleviated if the line emission were collimated. In the model of Rees & Meszaros (2000), where lines are produced by multiple scattering off the walls of an evacuated funnel along the rotation axis of the collapsing star, there can indeed be some collimation of the emission, enhancing its observed flux. The importance of this effect was however shown to be not too significant by Ghisellini et al. (2002). In particular, they found that, if the main scattering opacity within the funnel is provided by free electrons, then photons scattered deeper in the funnel will be lost, and the resulting line amplification can be at most a factor of 2. On the other hand, if the line under consideration is a resonant line, these photons may be rescattered by ions in the funnel wall and redirected towards the open space. In this case, line amplification can get up to a factor of 10 for an opening angle of the funnel of  $\sim 5$  deg (and it gets smaller for larger angles). Therefore, even under the most favorable circumstances, the required luminosity of the continuum has to be  $\gtrsim 10^{45} - 10^{46}$  erg/s.

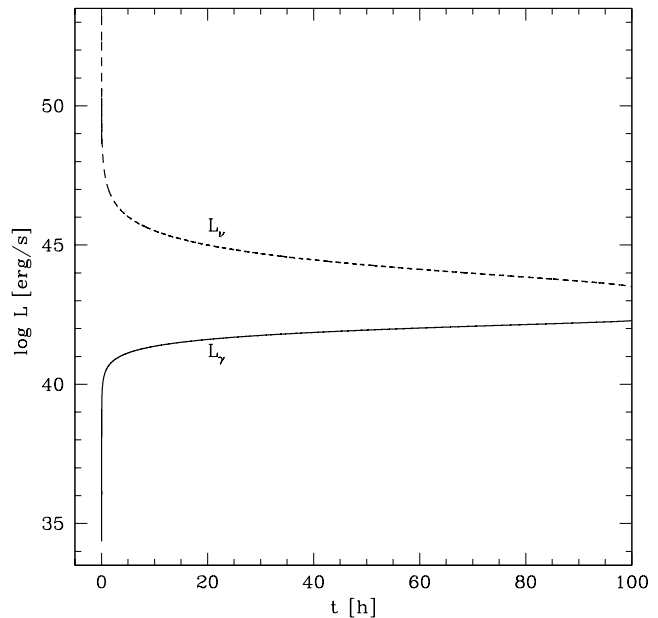


**Figure 7.** Long-term evolution of photon (solid line) and neutrino (dashed line) luminosities of the remnant torus, fed by the material fallback at its outer edge as in Eq. 18.

The issue therefore remains what is that provides the energy to power the lines.

The recent detection of a supernova associated with GRB 030329 (Stanek et al. 2003; Hjorth et al. 2003) gave strong support to the ideas that GRBs are the result of explosion of massive stars. In the collapsar model (MacFadyen & Woosley 1999), the remnant compact object is a black hole, and the “engine” is an accretion disc like the one we have studied here. The energy output at later times (i.e. after the GRB phase) is in this case given by the sluggish drain of orbiting matter into the newly formed black hole, after the supply of matter from the envelope of the collapsing star is exhausted. Our calculations allow us to evaluate the energy output from this remnant disc at the times (of the order of tens of hours) at which the emission features have been observed. Figure 7 shows the evolution of the photon and neutrino luminosities from the very early times of the GRB phase to several days after the GRB. While the neutrino luminosity drops following the decrease in the accretion rate (Figure 8), the photon luminosity increases with time. This is due to the decreasing photon opacity of the disc, which overcomes the decrease in energy flux that would be expected as a result of the declining mass accretion rate. The Rosseland mean opacity, calculated for the electron scattering and free-free transitions (see Equation 8) is very large in the initial disc, which is therefore almost totally opaque to photons ( $\kappa > 3 \times 10^2$  for  $r < 10R_s$ ). However, the opacity drops quickly and after  $\sim 10$  minutes it approaches the value of 0.4. Therefore as long as the main source of cooling is the neutrino emission, the photon luminosity rises with time. The trend will reverse when  $L_\nu < L_\gamma$  and the photon emission becomes the more important cooling mechanism (note however that advection is still very large). The

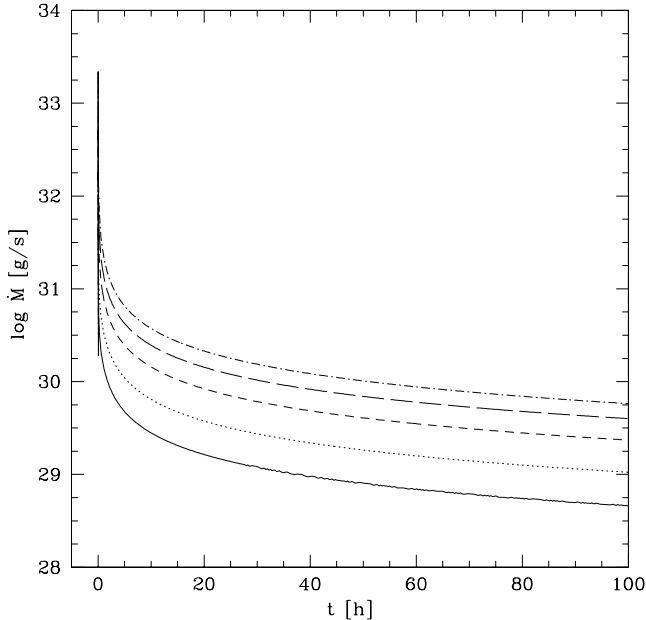


**Figure 8.** Long-term evolution of the accretion rate in the torus, plotted for several radii:  $5.27 R_S$  (solid line),  $9.85 R_S$  (dotted line),  $20.64 R_S$  (short-dashed line),  $35.37 R_S$  (long-dashed line) and  $46.1 R_S$  (dot-dashed line).

decreasing mass accretion rate will now result in lower and lower photon emission from the disc.

As the figure shows, at the times corresponding to the line observations, the photon luminosity is  $\sim 10^{41} - 10^{42}$  erg/sec, several orders of magnitude below what is required to produce the emission features at the observed luminosity level. The simulations in Figures 7 and 8 are performed for an initial accretion rate of  $1 M_\odot/s$ , but they give similar results for any initial value of  $\dot{M}$  that produce a GRB at early times. Since for higher initial accretion rates the neutrino cooling of the disc is even more effective, the photon luminosity at late times is lower: for  $2 M_\odot/s$  it is  $3.2 \times 10^{41}$  erg/s at  $t \sim 1$  day, while for  $1 M_\odot/s$  it was  $4.7 \times 10^{41}$  erg/s. The viscosity in the disc does not have a big impact on the long-term results either: the dissipation rate and the disc luminosity increase only slightly with  $\alpha$  and the change is of the order of  $\Delta \log L_\gamma = 0.3$  and  $\Delta \log L_\nu = 0.5$  when we change  $\alpha$  from 0.1 to 0.3. Therefore, our simulations imply that the energy output from the accretion disc alone is not sufficient to power the GRB emission lines (if these are indeed real).

An alternative possibility (Rees & Meszaros 2000) for producing a long-lasting energy output is by the collapse of a massive star into a fast millisecond pulsar (Usov 1994; Thompson 1994; Wheeler et al. 2000). In this case the late time energy is provided by the electromagnetic losses of the pulsar which, at a day after the burst, can easily be as high as  $10^{47}$  erg/s. Our results favor this scenario. Identification of the remnant compact object after the GRB explosion would provide an independent test of this scenario, and this should be possible in local galaxies after identification of GRB remnants (Loeb & Perna 1998; Efremov et al. 1998; Perna et al. 2000).

## 5 DISCUSSION

The bimodal distribution of durations of GRBs is most probably due to the different origin of the short and long bursts, and the proposed models of a GRB progenitor include binary mergers or collapse of a massive star. In both cases the formation of a dense accretion disc around a black hole is expected, and one of the possible ways of extracting the energy from the central engine is the neutrino-antineutrino annihilation. This process can give rise to the relativistic fireball, if the neutrinos convert into electron-positron pairs in the region of relatively low baryon density.

The merger scenario seems to be appropriate only in the case of short GRBs, of duration  $\lesssim 2$  seconds. Due to the need for a low baryon density above the poles, the favored case is black hole - neutron star merger. The neutron star can either be catastrophically disrupted in the first approach to the black hole or transfer mass to the BH 2 or 3 times, depending on the initial mass ratio. In either case in the end it forms a torus, whose mass is between  $0.25$  and  $0.7 M_\odot$ , and accretion rate of several  $M_\odot/s$ . Therefore the accretion time is of order of  $0.1 - 1.5$  sec (Janka et al. 1999).

In the collapsar scenario the black hole formation may be accompanied by a fallback of material, which over a period of minutes to hours feeds the accretion disc. If the initial accretion rate is sufficiently high to establish a dense disc cooled by neutrinos ( $\dot{M} \geq 0.1 M_\odot/s$ ), the powerful, long GRB may be produced.

The neutrino annihilation is most efficient near the rotation axis (Jaroszynski 1993). This process is able to account for the energy released in GRBs if a moderate beaming,  $\Omega/2\pi \sim 10^{-2}$ , is involved (Ruffert & Janka 1999). In this case the isotropised energy of a burst is of the order of  $10^{51} - 10^{52}$  erg/s. The jet collimation mechanism is possible e.g. due to the neutrino-driven wind, which can be expected from the outer disc regions if the neutrino luminosity is  $L_\nu > 10^{52}$  ergs/s and the estimated wind power is  $L_w = 2 \times 10^{49} (L_\nu/10^{52})^{(16/5)}$  (Rosswog & Ramirez-Ruiz 2003).

In addition to the fraction of accretion energy that goes into the jet via neutrinos, the energy extraction from the central engine is possible via magnetic fields (Blandford & Znajek 1977; Meszaros & Rees 1997; Kluźniak & Ruderman 1998). In this case, isotropic luminosities as high as  $10^{52} - 10^{53}$  erg/s are possible, even without beaming. The burst energy can also be increased due to the effects associated with the Kerr metric of a rotating black hole.

Here we start our calculations when the accretion disc has already established its quasi-steady state and evolves in the viscous timescale. We neglect the first, very violent stage of the disc formation, during which the material within a free fall time settles on the equatorial plane. The centrifugal force is balanced by gravity and the torus forms with a surrounding accretion shock. Inside this shock the temperatures and densities are high enough to provide enhanced neutrino emission during a few seconds before the disc formation (MacFadyen & Woosley 1999).

We computed the time dependent evolution of the accretion disc believed to be the GRB central engine. Our simulations took into account a physical equation of state, including gas and radiation pressure as well as the pressure from degenerate electrons. We calculated the energy balance



between the viscous heating and neutrino losses due to thermal processes and neutronization, in both optically thin and thick regimes. We also took into account the advective and radiative cooling. Time-dependent 2D hydrodynamical simulations of an accretion disc in GRBs have recently been calculated by Lee & Ramirez-Ruiz (2002), Lee et al. (2004) and Setiawan et al. (2004). Here we use the vertically integrated equations and the simulations are one-dimensional, which on one hand results in a great simplification of the problem, but on the other hand allows us to get insight into the various physical processes that act during the disc evolution. The most valuable aspect of such an approach is the possibility to study the long-term evolution of the remnant disc, especially in the frame of a long burst (collapsar) scenario.

The short bursts are powered by the neutrino cooled accretion disc, which exists for about  $\sim 2$  seconds. At this phase the neutrino luminosity remains very high during the first  $\sim 1 - 1.5$  seconds, while dropping as soon as the whole disc becomes advection dominated. In case of the long bursts, the fallback of material that occurs during the accompanying supernova explosion plays an essential role. The neutrino luminosity remains very high during the first 2-3 seconds of the burst, and then drops exponentially, being sufficiently high to feed the GRB during several tens of seconds.

The hyper-accreting, neutrino cooled disc is in either case very opaque to photons and the photon luminosity is always negligible whenever the neutrino emission is significant. However, as the disc evolves and the neutrino cooling becomes less efficient, the disc opacity due to electron scattering and free-free transitions decreases, thus allowing more and more photons to escape. Therefore the photon luminosity rises in time up to the level at which it exceeds the decreasing neutrino luminosity. Later on, since the disc is cooled mainly by photons (and advection), and during its evolution the accretion rate and energy generation decrease, the photon luminosity drops with time.

This stage of significant photon emission from the disc is extremely short and therefore not very important in case of the binary merger model. However, in the collapsar scenario it is much more extended in time and can last over several days to weeks, depending on the initial accretion rate and viscosity (the greater initial  $\dot{M}$  and  $\alpha$ , the longer the photon emission phase). Our calculations allow us to determine the residual level of photon luminosity from the disc at the times ( $\sim$  tens of hours) corresponding to the claimed observations of X-ray emission features in a few GRBs.

The emission from the disc could in principle power the emission lines, if the luminosity were sufficiently high. However, in our model this would require quite low initial accretion rates and an extremely high value of the viscosity parameter in the disc (for  $\alpha > 0.9$  and  $\dot{M} = 0.1M_{\odot}/s$  we could expect the X-ray luminosity of the order of  $10^{44}$  erg/s), whereas for a standard value of viscosity  $\alpha = 0.1$ , which is commonly adopted, the disc alone is not capable to power the lines. Therefore our simulations would rather favor the possibility of a long-lasting energy release by the electromagnetic losses of a newly born millisecond pulsar.

## ACKNOWLEDGMENTS

We thank Susumu Inoue, Andrea Merloni, Thomas Janka, Marek Sikora and Tomek Bulik for helpful discussions. This work was supported in part by the Gamma Ray Burst Training Network and by grants 2P03D00322 and PBZ 057/P03/2001 of the Polish State Committee for Scientific Research.

## REFERENCES

- Abramowicz M.A., Czerny B., Lasota J.-P., Szuszkiewicz E., 1988, *ApJ*, 332, 646
- Abramowicz M.A., Kato S., 1989, *ApJ*, 336, 304
- Antonelli L.A., et al., 2000, *ApJ*, 5454, L39
- Blandford R.D., Znajek R.L., 1977, *MNRAS*, 179, 433
- Chevalier R.A., 1989, *ApJ*, 346, 847
- Di Matteo T., Perna R., Narayan R., 2002, *ApJ*, 579, 706
- Drenkhahn G., Spruit H., 2002, *A&A*, 391, 1141
- Eichler D., Livio M., Piran T., Schramm D.N., 1989, *Nature*, 340, 126
- Efremov Y.N., Elmegreen B.G., Hodge P. W. 1998, *ApJ*, 501, L163
- Fox D. W. et al. 2003, *Nature*, 422, 284
- Ghisellini G., Lazzati D., Rossi E., Rees M.J. *A&A*, 389, L33
- Hannestad S., Raffelt G., 1998, *ApJ*, 507, 339
- Hjorth J., 2003, *Nature*, 423, 87
- Itoh N., Adachi T., Nakagawa M., Kohyama Y., Munakata H., 1989, *ApJ*, 339, 354
- Janiuk A., Czerny B., Siemiginowska A., 2002, *ApJ*, 576, 908
- Janka T., Eberl T., Ruffert M., Fryer C., 1999, *ApJ*, 527, L39
- Jaroszynski M., 1993, *Acta Astron.*, 43, 183
- Kluźniak W., Ruderman M., 1998, *ApJ*, 505, L113
- Kohri K., Mineshige S., 2002, *ApJ*, 577, 311
- Kouvelietou C., et al., 1993, *ApJ*, 413, L101
- Lazzati D., Ghisellini G., Celotti A., Rees M.J., 2000, *ApJ*, 529, L17
- Lazzati D., Ramirez-Ruiz E., Rees M. J. 2002, *ApJ*, 572L, 57
- Lee W.H., Ramirez-Ruiz E., 2002, *ApJ*, 577, 893
- Lee W.H., Ramirez-Ruiz E., Page D., 2004, *ApJ*, 608, L5
- Lightman A.P., Eardley D.M., 1974, *ApJ*, 187, L1
- Loeb A., Perna R., 1998, *ApJ*, 533, L35
- Lyutikov M., Blandford R. (astro-ph/0312347)
- MacFadyen A. I. & Woosley S. E. 1999, *ApJ*, 524, 262
- MacFayden A.I., Woosley S.E., Heger A., 2001, *ApJ*, 550, 410
- Meszaros P., Rees M.J., 1997, *ApJ*, 482, L29
- Muchotrzeb B., Paczyński B., 1982, *Acta Astron.*, 32, 1
- Narayan R., Paczyński B., Piran T., 1992, *ApJ*, 395, L83
- Narayan R., Piran T., Kumar P., 2001, *ApJ*, 557, 949
- Paczynski B., Bisnovatyi-Kogan G., 1981, *Acta Astron.*, 31, 283
- Paczynski B., 1986, *ApJ*, 308, L43
- Paczynski B., 1991, *Acta Astron.*, 41, 257
- Paczynski B., 1998, *ApJ*, 494, L45
- Perna R., Raymond J., Loeb A. 2000, *ApJ*, 533, 658
- Piro L., et al., 1999, *ApJ*, 514, L73

- Piro L., et al., 2000, *Science*, 290, 955  
Popham R., Woosley S.E., Fryer C., 1999, *ApJ*, 518, 356  
Pringle J.E., Rees M.J., Pacholczyk A.G., 1974, *A.&A.*, 29, 179  
Qian Y.Z., Woosley S.E., 1996, *ApJ*, 471, 331  
Rees M.J., Meszaros P., 1994, *ApJ*, 430, L93  
Rees M.J., Meszaros P., 2000, *ApJ*, 545, L73  
Reeves J.N., et al., 2002, *Nature*, 416, 512  
Rosswog S., Liebendörfer M., 2003, *MNRAS*, 342, 673  
Rosswog S., Ramirez-Ruiz E., 2003, *MNRAS*, 343, L36  
Rosswog S., Speith R., Wynn G.A., 2004, *MNRAS*, 351, 1121  
Ruffert M., Janka T., 1999, *A&A*, 344, 573  
Ruffert M., Janka T., Schäfer G., 1996, *A&A*, 311, 532  
Setiawan S., Ruffert M., Janka H.-Th., 2004, *MNRAS*, in press (astro-ph/0402481)  
Shakura N.I., Sunyaev R.A., 1973, *A.&A.*, 24, 337  
Sikora M., Begelman M.C., Coppi P., Proga D., 2003, *ApJ* submitted (astro-ph/0309504)  
Stanek K.Z., et al., 2003, *ApJ*, 591, L17  
Stern B., 2003, *MNRAS*, 345, 590  
Thompson C., 1994, *MNRAS*, 270, 480  
Turner N.J., 2004, *ApJ*, 605, L45  
Usov V.V., 1994, *MNRAS*, 267, 1035  
Wheeler J.C., Yi I., Höflich P., Wang L. 2000, *ApJ*, 537, 810  
Woosley S.E., 1993, *ApJ*, 405, 273  
Yoshida A., et al. 1999, *A&AS*, 138, 433  
Zhang B., Meszaros P., 2003, *International Journal of Modern Physics A*, in press (astro-ph/0311321)